Ab initio study of silver bromide Ag[sub n]Br[sub p][sup (+)] clusters (n≤6,p=n,n–1)

F. Rabilloud, F. Spiegelman, J. L'hermite, P. Labastie

Ab initio study of silver bromide $Ag_nBr_p^{(+)}$ clusters ($n \leqslant 6, p=n, n-1$)

F. Rabilloud
Laboratoire CAR (UMR 5589 CNRS-UPS), IRSAMC, Université Paul Sabatier, 118 Route de Narbonne, F31062 Toulouse Cedex 4, France

F. Spiegelman
Laboratoire de physique quantique (UMR 5626 CNRS), IRSAMC, Université Paul Sabatier, 118 Route de Narbonne, F31062 Toulouse Cedex 4, France

J. M. L'Hermite and P. Labastie
Laboratoire CAR (UMR 5589 CNRS-UPS), IRSAMC, Université Paul Sabatier, 118 Route de Narbonne, F31062 Toulouse Cedex 4, France

(Received 14 December 1999; accepted 3 October 2000)

Ab initio calculations in the framework of the density functional theory (DFT) with 19-electron pseudopotential on silver atoms are performed to study the lowest-energy isomers of silver bromide clusters $Ag_nBr_p^{(+)}$ ($n \leqslant 6$, $p=n$, $n-1$). The stability, the structural and electronic properties of neutral, and positively charged systems are examined. The B3LYP functional has been used. For the smallest species, the DFT/B3LYP results are very close to those obtained with multireference configuration interaction or coupled cluster methods. In Ag_nBr_{n-1} clusters, the excess electron density shows a picture intermediate between that observed in alkali halide clusters (F-center or localization on a pending alkali atom) and that suggesting partial delocalization on a dimer or trimer silver subunit. Isomer stabilities, fragmentation energies, electric dipole moments, adiabatic and vertical ionization potentials are calculated. The use of 11-electron pseudopotential on silver is discussed. © *2001 American Institute of Physics.* [DOI: 10.1063/1.1328396]

I. INTRODUCTION

Small clusters often present significant physical and chemical differences with respect to both the molecule and the bulk phase. The evolution of the properties with cluster size is a major challenge which has become a field of intensive research both for experimentalists and theoreticians.

Mixed clusters have been the object of recent interest. Among them, alkali halides have received substantial experimental and theoretical attention. Their ionic bonding character has allowed the development of simple models to study the interaction between ions. In particular, the structural and electronic properties of the stoichiometric M_nX_n systems as well as the nonstoichiometric M_nX_{n-1} have been investigated. It has been observed that the excess electron in M_nX_{n-1} may either be localized (in an anion defect location, also known as the F-center, or on an extra alkali atom), or semi-localized (in various defects such as corners, edges, steps, or irregular vacancies) or even widely delocalized.[1–4]

The *ab initio* study of ionic clusters involving noble metal atoms is less simple because of the presence of *d* electrons, but it is also of significant interest. In particular, silver bromide has been highly used for its optical properties in photography. Experimental investigations have shown that the growth of small silver clusters on AgBr microcrystals has a crucial role in the photosensitization process.[5] The electronic properties occurring with small silver microclusters have also been studied in solutions.[6] Various theoretical works[7–11] have been concerned with the energetics and electronic properties of small silver or mixed gold/silver clusters adsorbed on surfaces and have discussed the role of size.

Until very recently, no theoretical study was available to our knowledge on small free silver bromide clusters. In a previous paper,[12] we have reported an *ab initio* configuration interaction (CI) study for small $Ag_nBr_p^{(\pm)}$ clusters ($n,p \leqslant 2$) in which we analyzed the structural and electronic properties of neutral and ionic clusters explicitly treating 19 electrons on silver and 7 electrons on bromine. Unfortunately, computations of geometries or others properties via *ab initio* CI quantum chemical methods are hardly extensible to larger systems, because of their power dependence with the number of electrons. To investigate larger clusters, one can try to develop empirical models to describe the interactions between the constituting atoms. Model potentials were early developed to study solid state properties and surface defects. The range of validity and the limitations of additive pairwise potentials combined with the shell model were discussed.[13] Further works examined the improvements brought by the inclusion of three-body potentials.[14–16]

We have shown in our previous *ab initio* work that, although the stability of those small clusters could mainly be associated with electrostatic interactions, distortions were found from the geometries that could be expected with the simplest pair-additive Coulomb ionic model. For instance, Ag_2Br_2 was calculated to be a rhombus and not a square. Ag_2Br^+ turned out to be bent and not linear. Such distorsions are attributable to several, sometimes convergent causes. The most straightforward contribution is that induced by polarization forces. In the case of silver bromide, one may expect significant distortions due to the inequivalent polarizabilities

of the silver cation and of the bromine anion. Thus the polarization forces tend to maximize the local electrostatic fields on the more polarizable ions, namely the bromine anions. This is a possible interpretation of the trend to bending observed in Ag_2Br_2 and Ag_2Br^+. However, other contributions can also be invoked. One is the extra short-distance repulsion forces between the ions due to the Pauli principle which usually scale according to the sizes of the ions. Finally, another important contribution involves the amount of charge transfer, namely the balance between purely ionic and iono-covalent character. This latter balance is clearly related with the significant overlaps between the $4p$ atomic orbitals of bromine and the $4d$ of silver. The results obtained for $Ag_nBr_p^{(\pm)}$ clusters with $n,p \leqslant 2$ should be extended to larger sizes in order to provide more thorough insight in the bonding.

The development of Density Functional Theory (DFT) calculations over the last few years has proved that DFT methods may provide satisfactory results for a reasonable computational cost. They allow calculation of some properties, particularly the geometrical structures of large systems for which CI calculations are still too heavy. Very recently, this approach was used to study stoichiometric silver halide clusters. Zhang *et al.*[17] investigated neutral stoichiometric silver halide clusters with $n \leqslant 9$ in the framework of all-electron calculations and the B3P86 functional. While the final energy of the proposed isomers was carried out with extended basis sets, the search of the geometries only involved rather small basis sets such as 3-21G on silver and 3-21G* on bromine. Moreover, no account of relativistic effects was mentioned. In a review paper, Srinivas *et al.*[18] published DFT/B3LYP calculations on neutrals and singly ionized stoichiometric clusters ($n \leqslant 4$) using the 19-electron pseudopotential of Hay and Wadt[19] and a $3s3p2d$ basis set on silver.

In the present paper, we present a DFT study of the lowest-energy isomers of silver bromide clusters involving both stoichiometric Ag_nBr_n and nonstoichiometric Ag_nBr_{n-1} clusters with an excess metal atom. Both neutral and singly ionized clusters are investigated. We have considered sizes up to $n=6$. In order to derive reliable reference results we have performed DFT calculations with pseudopotentials involving 19 explicit electrons on silver and 7 electrons on bromine as in our previous CI study. Those pseudopotentials include averaged relativistic effects which are relevant for bromine and silver. We also use large basis sets than in the previous investigations. Details of the calculations are introduced in Sec. II. In Sec. III, we first compare on dimers, trimers, and tetramers the ability of B3LYP/DFT calculations to reproduce CI type calculations, namely the MRPT2 results published previously and also new coupled cluster type calculations which we provide in the present work. We then perform DFT/B3LYP studies of properties for the larger clusters including structures, stabilities, dissociation energies, adiabatic and vertical ionization potentials, and static electric dipole moments. We also examine the validity of using pseudopotentials involving 11 explicit electrons only, the $4s$ and $4p$ electrons being kept in the core. Such approach was indeed used recently on small pure silver clusters and silver oxide clusters where the relationship between shape and electronic spectra was discussed.[20,21]

We summarize the results in Sec. IV and emphasize the geometrical and bonding features of the lowest isomers of neutral and singly charged species. We examine the relationship with the electronic structure and the nature of the orbitals, with particular attention to electron localization in clusters with one excess electron. The stabilities and fragmentation patterns are commented in light of recent experimental results. Comparison with the theoretical investigations of the abovementioned authors is also given.

II. CALCULATIONS

Both Ag and Br atoms were represented through relativistic effective core pseudopotential (RECP). In the small core pseudopotential (SCP) version, silver was considered an $[Ag^{19+}]$ core with $4s$, $4p$, $4d$, and $5s$ active electrons[22] as in our previous work.[12] In the large core pseudopotential (LCP) version, an $[Ag^{11+}]$ pseudopotential[23] determined from both $d^{10}s^1$ and d^9s^2 situations was used. Bromine was described with a $[Br^{7+}]$ core with $4s$ and $4p$ active electrons.[24] Calculations were achieved in the linear combination of atomic orbitals (LCAO) scheme. For the small core pseudopotential calculation, the Gaussian basis set on silver was $8s7p6d$ contracted into $6s5p3d$. The influence of an extra f function, with exponent 1.3 from Ref. 25, was checked. For the large core pseudopotential calculation, a $5s3p5d$ set contracted into $3s2p3d$ was used. In both cases a $5s6p1d$ contracted into $3s3p1d$ was used on bromine.

For all clusters the electronic calculations performed in the framework of the density functional theory used the GAUSSIAN98 package[26] and the hybrid B3LYP functional which involves Becke's three-parameter exchange functional.[27]

In order to complement the CI data corresponding to our previous work and to allow for small core versus large core comparison within this framework, we have achieved for dimers large core and small core coupled cluster calculations using the version involving single and double substitutions (CCSD) and also the CCSD(T) approximation taking into account the effect of triple substitutions. On trimers and tetramers we could only perform large core coupled cluster calculations involving double excitations uniquely (CCD). Those large core calculations can be compared with small core calculations using a multi-reference CI plus second-order Moller–Plesset perturbation scheme hereafter labeled MRPT2[12] instead of the coupled cluster scheme, too heavy to be achieved with 19 electrons per silver atom.

In all cases, the optimization process was carried out using gradient algorithms starting in each case with sets of guessed isomer structures predetermined with an empirical electronic+polarization model and also with structures already known for alkali halide systems[3,28–30] or other silver complexes.[31] Moreover, systematic crossed searches were carried out starting either from LCP or SCP geometries and also starting from geometries obtained for various charges and stoichiometries. All optimizations were carried on without symmetry constraints (C_1 symmetry group). In the dis-

TABLE I. Equilibrium distances (r_e in a_0) and dissociation energies (D_e in eV) of dimers. Two pseudopotentials on silver are compared. The Gaussian atomic basis set includes one *f* function on silver, except in B3LYP* calculations.

		$[Ag^{19+}]$ core				$[Ag^{11+}]$ core			
Species		MRPT2	CCSD(T)	B3LYP	B3LYP*	CCSD(T)	B3LYP	B3LYP*	Expt.
Ag_2	r_e	4.78	4.84	4.90	4.91	4.77	5.16	5.16	4.78[a]
	D_e	1.96	1.64	1.54	1.52	1.50	1.25	1.23	1.66[b]
AgBr	r_e	4.58	4.58	4.61	4.62	4.70	4.83	4.84	4.52[d]
	D_e	2.67	2.72	2.63	2.61	2.77	2.74	2.71	3.1[e]
$AgBr^+$	r_e	5.02	4.95	4.87	4.89	5.35	5.39	5.40	-
	D_e	0.89	0.87	1.01	1.00	0.55	0.56	0.55	1.41[f]
Br_2	r_e	4.42	4.38	4.40	4.40				4.31[c]
	D_e	2.01	1.71	1.92	1.92				1.99[c]

[a]Reference 32.
[b]Reference 33.
[c]Reference 34.
[d]Reference 35.
[e]Value of D_0^0: Ref. 34.
[f]Estimation of D_0^0: Ref. 36.

cussion, we report the lowest isomers obtained using 19- or 11-electron pseudopotentials.

The use of *f* type functions to polarize the *d* shell of Ag^+ is in principle suitable, although it consequently burdens the calculation. The role of polarization functions is known to be extremely important in Hartree–Fock plus CI calculations. The omission of the *f* function yields an overestimation of the CCSD(T) calculated equilibrium distances by 0.3 bohr on Ag_2, and 0.1 bohr on AgBr and $AgBr^+$, respectively. The corresponding dissociation energies are underestimated by 0.23 eV and 0.08 eV for Ag_2 and $AgBr^+$, respectively, while that of AgBr is overestimated by 0.05 eV. We present in Table I the CCSD(T) results for dimers involving the *f* function. It can be noticed that the use of an *f* function yields very small changes in the DFT/B3LYP scheme, either using small core or large core pseudopotentials (discrepancies less than 0.02 bohr for the equilibrium distances and 0.02 eV on the binding energies).

We have further checked for $Ag_nBr_n^{(+)}$ and $Ag_nBr_{n-1}^{(+)}$ with $n \leqslant 4$ the influence of using *f* functions on Ag atoms. The detailed comparison of geometries is shown in Table II for trimers and tetramers. Even for the largest clusters ($n=4$), no significant change was found as concerns the geometries (less than 0.02 bohr for the interatomic distances and almost no modification of the angles), changes less than 0.05 eV, for the total energies. For $n>4$, the calculations were carried on without *f* functions.

III. RESULTS AND DISCUSSION

A. Comparison between DFT and CI calculations

Table I lists the spectroscopic constants of dimers calculated in the CCSD(T) approximation and in the DFT/B3LYP scheme either using large core or small core pseudopotentials on Ag, as well as our previous MRPT2 results obtained with small core pseudopotentials. The B3LYP calculations are in satisfactory agreement with the CCSD(T) or MRPT2 results, whatever the pseudopotential used, except for the equilibrium distance of Ag_2 using large core pseudopotential for which the discrepancy is 0.4 bohr. The main effects of small core pseudopotential are to generally reduce the equilibrium distance [systematic with B3LYP, an exception for Ag_2 with CCSD(T)], and to increase the dissociation energy, except for AgBr. The effect is particularly large on the $AgBr^+$ cation since the dissociation energy goes from about 0.55 eV using large core pseudopotential to about 1 eV with small core pseudopotential, significantly improving the poor agreement of the former with the experimental value of 1.41

TABLE II. C_{2v} (or D_{2h}) symmetry optimized geometries of trimers and tetramers clusters. *d* is the Ag–Br bonding distance (in bohr), α is the $\widehat{AgBrAg}$ angle (in deg). Two pseudopotentials on sliver are compared. The Gaussian atomic set includes one *f* function on silver, except in B3LYP* and CCD* calculations.

	$[Ag^{19+}]$ core						$[Ag^{11+}]$ core							
	MRPT2		B3LYP		B3LYP*		CCD		CCD*		B3LYP		B3LYP*	
Species	*d*	α	*d*	α	*d*	α	*d*	α	*d*	α	*d*	α	*d*	α
Ag_2Br	5.00	61.0	5.07	61.7	5.07	61.4	5.12	57.8	5.20	62.1	5.27	63.5	5.28	63.4
Ag_2Br^+	4.80	111.0	4.79	111.6	4.79	111.6	4.87	121.6	4.98	129.6	5.04	127.9	5.04	128.0
Ag_2Br_2	5.10	69.2	5.00	65.6	5.01	65.4	5.05	69.2	5.14	71.1	5.20	71.6	5.20	71.3
$Ag_2Br_2^+$	4.97	80.2	4.89	82.6	4.90	82.7	5.24	104.4	5.36	110.7	5.38	107.3	5.39	105.9

TABLE III. Adiabatic ionization potential in eV of Ag, AgBr, Ag_2Br, and Ag_2Br_2. Two pseudopotentials on silver are compared. The Gaussian atomic set include one *f* function on silver, except in B3LYP* and CCD* calculations.

	$[Ag^{19+}]$ core			$[Ag^{11+}]$ core				
Species	MRPT2	B3LYP	B3LYP*	CCD	CCD*	B3LYP	B3LYP*	Expt.
Ag	7.16	7.97	7.97	6.67	6.40	6.92	6.92	7.58[a]
AgBr	8.84	9.60	9.58	8.75	8.59	9.10	9.08	9.26[b]
Ag_2Br	5.88	6.61	6.63	5.61	5.32	5.80	5.80	
Ag_2Br_2	8.78	8.98	8.98	8.78	8.60	8.66	8.66	

[a]Reference 37.
[b]Estimation, Ref. 36.

eV. For the other diatomics involving silver, the B3LYP 19-electron results are in satisfactory agreement with the experimental values. A good agreement is also obtained on Br_2.

The same consistency between B3LYP and CCD or MRPT2 results for a given pseudopotential can be also observed on the structural ground state of trimers and tetramers, as illustrated in Table II where the geometrical data are detailed. Ag_2Br and Ag_2Br^+ both have isosceles geometry in all the calculations and Ag_2Br_2 is a planar rhombus. The use of small core versus large core pseudopotentials does not yield strong morphological change, mainly a shortening of the bond distances, and a significant decrease of the apex angle for Ag_2Br^+. In contrast, an important difference is observed in the case of $Ag_2Br_2^+$. Indeed the large core pseudopotential calculations all yield a bent rhombus with the Ag–Ag diagonal longer than the Br–Br one (5.39 bohr with B3LYP, 5.84 bohr with CCD) and a deviation from planar situation resulting into a diedral angle around Br–Br of 17.7 degree with B3LYP, 17.7 degree with CCD. Oppositely, the calculations with small core pseudopotentials yield a Br–Br distance (7.36 bohr with B3LYP, 7.60 bohr with MRPT2) larger than the Ag–Ag one (6.47 bohr with B3LYP, 6.40 bohr with MRPT2). In the LCP case, the electron is removed from a σ_u-like molecular orbital localized on the bromine dimer. This results into a quasi Br_2^- unit stabilized by the Ag^+ cations, i.e., $Ag^+Br_2^-Ag^+$ (the B3LYP equilibrium distance of isolated Br_2^- is 5.61 bohr). In the SCP calculation, the electron is still removed from the bromine atoms, but which cannot any longer be considered as forming a dimer unit because of their separation. The situation can rather be analyzed as $Ag^+Br^{-1/2}Br^{-1/2}Ag^+$. In this latter case, the $4p$ orbitals of bromine preferably interact with the $4d$ shell of silver, rather than forming a bromine dimer anion. The Ag_2Br trimer has a $D_{\infty h}$ low lying isomer in the B3LYP calculations, 0.32 eV and 0.21 eV above the isosceles structure in SCP and LCP calculations, respectively. The AgBr distances in this isomer are 4.91 bohr (SCF) and 5.14 bohr (LCP), respectively.

Table III shows that the adiabatic ionization potentials calculated with the B3LYP/DFT scheme are generally larger than the CI values. The SCP IPs are systematically larger than the LCP ones, the differences ranging from 0.3 eV for Ag_2Br_2 up to 0.8 eV for Ag_2Br and 1 eV on the atomic silver. In the SCP case, the MRPT2 and B3LYP values frame the experimental IPs available on Ag and AgBr.

B. Lowest-energy structures and isomers

Structures of larger clusters were only obtained within the DFT framework. Unless explicitly stated, we always start in the following by the structures obtained with SCP calculations. However, we will also compare them to results obtained using LCP.

All the lowest SCP isomers of stoichiometric Ag_nBr_n clusters up to $n=6$ are planar or nonplanar cycles (Fig. 1). The lowest-energy structure of Ag_3Br_3 is quasi-triangular (D_{3h} symmetry) with the bromine at the apexes. Deviation from the hexagonal arrangement, which are expected in pure ionic systems, is large since the $Br\widehat{Ag}Br$ angles are 165 deg. The AgBr bond lengths are 4.81 bohr intermediate between that in the diatomic molecule (4.62 bohr) and those in Ag_2Br_2 (5.01 bohr). A similar lowest-energy structure was found using LCP with slightly different angles ($Br\widehat{Ag}Br$ angle of 152 deg) longer AgBr distances (5.08 bohr). A second LCP isomer [labeled (b) in Fig. 1 and Table IV] lying 0.55 eV above the former was obtained. It was, however, not found stable using SCP. We have tried to start the optimization with cubiclike geometries such as the bent or planar ladder, linear or quasi-linear geometries but those higher energy starting guess structures always converged to the same lowest quasi-triangular one, whatever the pseudopotential used.

Three stable isomers were obtained for Ag_4Br_4. The lowest one (a) has a squarelike shape here also with the bromine at the apexes. It is significantly bent around a Br–Br diagonal with an diedral angle of 148 deg (C_{2v} symmetry). The BrAgBr side atoms are almost aligned and the AgBr bond lengths are 4.78 bohr, very close to those found in Ag_3Br_3. The Ag–Ag distances are 6.65 bohr and the $Ag\widehat{Br}Ag$ angles are 88 deg. A second isomer (b) with C_s symmetry lies at 0.85 eV above the squarelike structure. It consists of an AgBr tail folded above an Ag_3Br_3 (a) cluster and connected to one of the Br apexes. The Ag_3Br_3 basis is slightly deformed with respect to the free cluster. The bond length of the terminal AgBr tail fragment is 4.60 bohr, significantly shorter than the AgBr distances in the Ag_3Br_3 basis plane (in the range 4.80–4.98 bohr). This BrAgBr tail is quasi-linear. The folding angle (72 deg) is such that the closest neighbor Ag–Ag distances are almost all equal (5.87 bohr). Finally a T_d symmetry isomer (c) was obtained at 1.07 eV above the isomer (a). It can be considered as a distorted

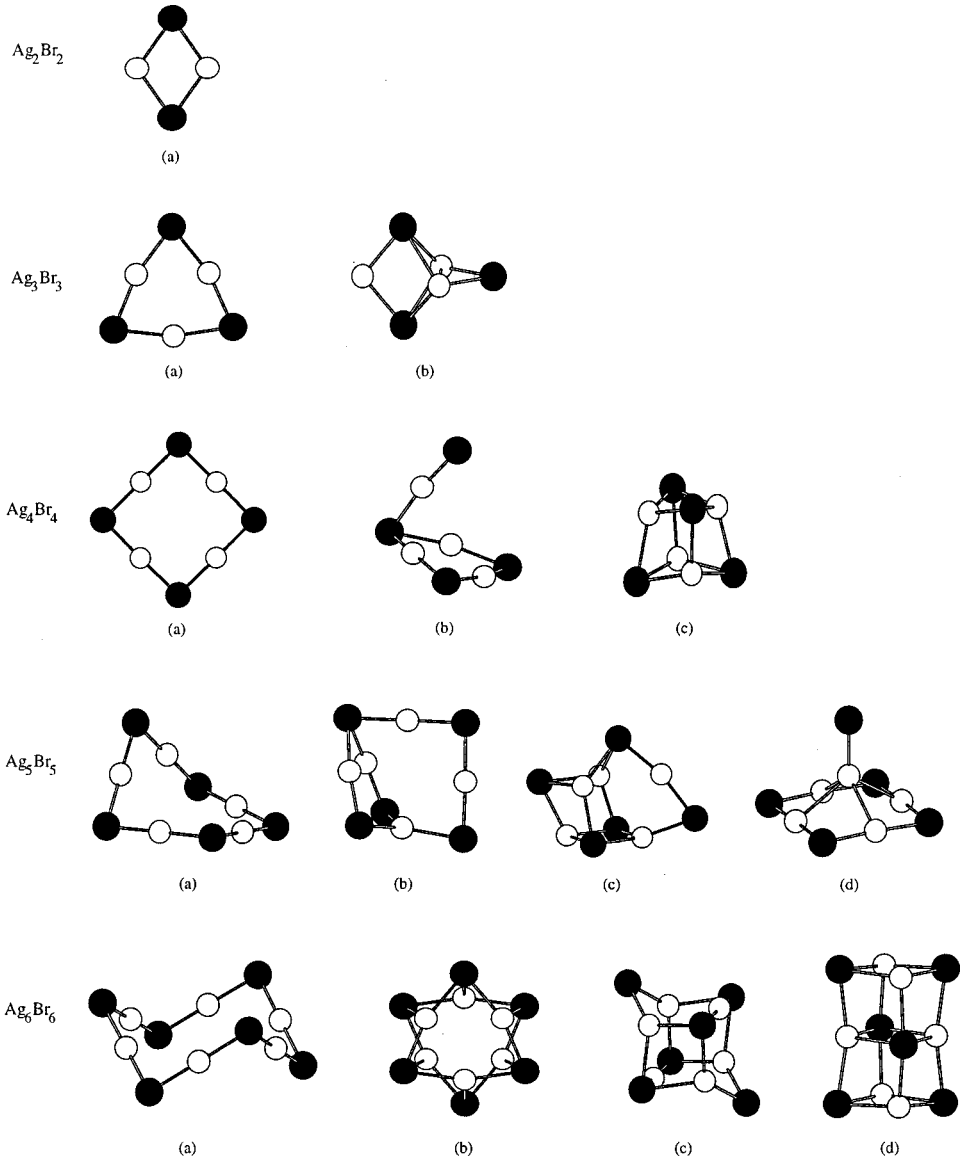

FIG. 1. Optimal geometries of neutral Ag_nBr_n clusters. The small white spheres represent silver atoms, the large dark spheres represent bromine atoms.

cube with the bromine atoms pointing outward. The AgBr distances are 5.26 bohr. The Ag–Ag and Br–Br distances are 5.94 bohr and 8.43 bohr, respectively. As for Ag_3Br_3, no linear nor quasi-linear structure was found to be stable. Isomers (a) and (c) were also found stable using LCPs. The important difference is that the LCP's isomer (c) is lower than isomer (a) by 0.31 eV. The AgBr distances are systematically longer [5.05 for isomer (a) and 5.42 bohr for isomer (c)] with LCP's than when using SCPs.

The trend that favors cyclic arrangements still applies for the larger sizes. The lowest isomer (a) for Ag_5Br_5 is a nonplanar distorted pentagon with Br apexes and BrAgBr sides having different $\widehat{AgBrAg}$ angles (respectively, 89, 95, 99, 98, and 92 deg around the cycle). All the AgBr bond distances were found strictly equal (4.77 bohr). Similarly, Ag_6Br_6 is a nonplanar distorted hexagon with BrAgBr sides. It can be considered as a trans-deformed complex of the hexagon retaining the C_{3v} symmetry. All of the $\widehat{AgBrAg}$ angles are identical (94 deg) and such are the AgBr bond lengths (4.77 bohr). For both $n=5$ and $n=6$, the higher isomers can be viewed as grown around intricated building triangular Ag_3Br_3 and square Ag_4Br_4 units, actually deformed but retaining the basic units connectivity. One characteristic example is Ag_5Br_5 (b) which is located 0.52 eV above structure (a) and includes two deformed square cycle and one deformed triangle. Other remarkable examples are Ag_5Br_6 (c) with an AgBr dimer deposited on a square basis (C_{4v} symmetry) and Ag_6Br_6 (b), 0.21 eV above isomer (a), which consists of two superimposed twisted Ag_3Br_3 subunits with global D_{3d} symmetry. For $n=5$, only isomers (a), (b), and (c) exist as stable minima when using LCP's; that with the lowest energy is isomer (c), below isomers (a) and (b) by 0.44 and 0.68 eV, respectively. For $n=6$, only isomers (a) and (b) are found to be stable, and the LCP order is again reversed [(b)$<$(a) by 0.14 eV]. An extra deformed parallepipedic stable structure is found (which does not exist with SCP) and is degenerate with isomer (a).

From a practical point of view, computations of $Ag_nBr_n^+$ ionic clusters optimizations turned out to be more difficult than those on neutral stoichiometric species. The chemical bonding is no longer totally ionic and the presence of an

TABLE IV. Symmetry and relative energies (in eV) for neutral clusters B3LYP optimized structures using two core pseudopotential on silver. A dash means that the structure is not a minimum.

Cluster		Symmetry	$[Ag^{19+}]$	$[Ag^{11+}]$
Ag_2Br_2	a	D_{2h}	0.00	0.00
Ag_3Br_3	a	D_{3h}	0.00	0.00
	b	C_{2v}	-	0.55
Ag_4Br_4	a	C_{2v}	0.00	0.31
	b	C_s	0.85	-
	c	T_d	1.07	0.00
Ag_5Br_5	a	C_1	0.00	0.44
	b	C_s	0.52	0.68
	c	C_s	0.75	0.00
	d	C_{4v}	0.93	-
Ag_6Br_6	a	C_{3v}	0.00	0.14
	b	D_{3d}	0.21	0.00
	c	C_{2v}	0.28	-
	d	D_{2h}	-	0.14
Ag_2Br	a	C_{2v}	0.00	0.00
	b	$D_{\infty h}$	0.31	0.21
Ag_3Br_2	a	C_{2v}	0.00	0.00
	b	C_s	0.72	0.30
Ag_4Br_3	a	$C_{3v}-C_s$[a]	0.00	0.05
	b	C_{2v}	0.31	0.27
	c	C_{3v}	0.73	0.00
Ag_5Br_4	a	C_{4v}	0.00	0.15
	b	C_s-C_{2v}[b]	0.54	0.46
	c	C_{2v}	1.26	0.00
	d	C_{3v}	1.57	0.15

[a]The structure of Ag_4Br_3 (a) has C_{3v} symmetry using the $[Ag^{19+}]$ core pseudopotential. With the $[Ag^{11+}]$ core pseudopotential, the symmetry is C_s.

[b]The structure of Ag_5Br_4 (b) is planar using the $[Ag^{11+}]$ core pseudopotential (C_{2v} symmetry). With the $[Ag^{19+}]$ core pseudopotential, the geometry is not planar and the symmetry is C_s.

open shell seems to make convergency of both SCF and geometrical optimizations more tedious. Thus we have limited our search for size $n \leqslant 4$.

Up to that size, the removal of one electron essentially yields the lowest structures which resemble those of the neutrals with various generally small deformations (Fig. 2 and Table V). The $Ag_2Br_2^+$ case was already analyzed in our previous paper at the MRPT2 level.[12] As quantitatively illustrated higher, the present B3LYP/DFT result is consistent with the former. The cluster remains a rhombus with lengthening of the Ag–Ag distance (6.37 bohr) with respect to the neutral cluster (5.41 bohr), the electron being removed from the b_{2u}HOMO which is essentially an antibonding combination of the $4p$ atomic orbitals of the bromine atoms along the Br–Br axis. This simulatenously reduces the antibonding character between the bromine atoms as well as their electrostatic repulsion. It also reduces the screening due to the HOMO between the silver atoms. Consequently, the $\widehat{AgBrAg}$ angle opens from 65 to 83 deg. The AgBr bond lengths are slightly reduced from 5.00 bohr to 4.90 bohr. A second chainlike isomer is found lying 0.13 eV above the former. It is not linear (C_s symmetry), the terminal BrAg segment having an $\widehat{AgBrAg}$ angle of 109 deg. The electron spin density is 0.83 on the terminal bromine showing that this cluster can be mainly described as $(AgBrAg)^+Br$. The geometry of $(AgBrAg)^+$, with AgBr distances of 4.80 and 4.75, is very close to that of free Ag_2Br^+ (112 deg for the angle and 4.79 bohr for the AgBr bond length). Both isomers exist when using LCPs. However, the geometry of isomer (a) is significantly changed since the Br atoms become as close as 5.40 bohr whereas the Ag–Ag distance is 8.60 bohr, inverting the short and long diagonal of the rhombus with respect to the SCP result.

The HOMO level of Ag_3Br_3 is doubly degenerate and corresponds to an out-of-plane orbital with e'' symmetry. However, another level (associated with two in-plane e' orbitals) is quasi-degenerate with the HOMO level (degeneracy within 10^{-4} hartree). As a consequence, the removal of the electron induces a Jahn–Teller effect. The lowest-energy isomer (a) corresponds to a $D_{3h} \rightarrow C_{2v}$ symmetry lowering, stabilizing state $^2B_2$. The relayed geometrical configuration is associated with a shortening of one Ag–Ag distance (5.40 bohr) and a increase of the others (6.98 bohr). The AgBr lengths remain close to their value in the neutral cluster. There is a second isomer 0.43 eV above the former with a quite different topology. A peculiar feature is that it exhibits a short Br–Br distance (5.72 bohr) comparable to that of Br_2^- (5.61 bohr). This latter structure is the lowest one when using LCPs.

Whereas Ag_4Br_4 was moderately deformed from a square structure, $Ag_4Br_4^+$ is planar and has D_{4h} symmetry. The HOMO of the neutral cluster is nondegenerate and the removal of the electron increases the repulsion between the edge silver atoms which rationalizes the flattening of the cluster. The electronic state has $^2B_{2u}$ symmetry. The next isomer (b) is 0.47 eV higher and has $^2A''$ symmetry. It is clearly related to the neutral isomer (b). The missing electron is removed from the terminal bromine atom of the tail. This results into a larger angle between the tail segment and the plane (109 deg). Finally, isomer (c) results from a distortion of neutral isomer (c) due to a Jahn–Teller effect since the HOMO of the latter is three-fold degenerate. The electron is removed from two bromine atoms, and the corresponding rhomboidal face almost transforms into a slightly bent square. The symmetry is lowered from T_d to C_{2v} and the electronic state is $^2B_2$. This evolution is very similar to the situation in $Ag_2Br_2^+$ where, due to the unscreening, the Br–Br distance is shortened. Again the LCP calculation in which isomer (c) is the lowest fails to reproduce the correct isomer order.

We now discuss the singly charged nonstoichiometric clusters $Ag_nBr_{n-1}^+$ (Fig. 3 and Table V). Comparison can be made with previous calculations concerned with some alkali halides clusters, namely $Na_nF_{n-1}^+$,[28] $Na_nI_{n-1}^+$, or $Cs_nI_{n-1}^+$.[30]

Ag_2Br^+ is an obtuse triangle with an apex angle of 112 deg. As in our previous study,[12] this structure differs from that of the M_2X^+ alkali halide trimer which has a linear $D_{\infty h}$ symmetry. The larger polarizability of Br^- versus that of Ag^+ tends to bend the cluster in order to maximize the electrostatic field on bromine. However, analysis of the two highest a_1 orbitals shows a propension for three-body bonding mixing involving the $4p$ orbitals of Br and the $4d$ orbitals of Ag, mixing which is clearly favored by bending. Simultaneously the $4p$ orbitals pointing along the C_2 axis

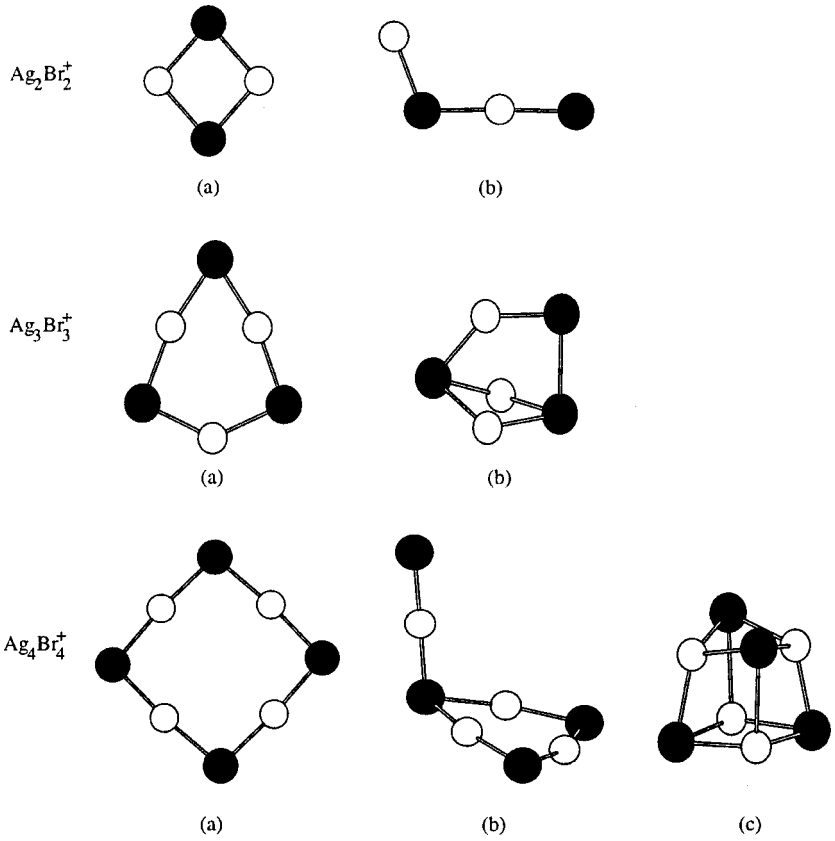

FIG. 2. Optimal geometries of cationic $Ag_nBr_n^+$ clusters. The small white spheres represent silver atoms, the large dark spheres represent bromine atoms.

screens the positive charges on the silver atoms.

Isomer (a) of $Ag_3Br_2^+$ is an alterant extension of the previous unit. We have checked the fully linear geometry and a W-shape chain where both terminal silver atoms are on the same side. None of them were found stable, converging toward geometry (a). The linear chain is a stable minimum only with LCPs. Two others isomers were obtained, one (b) is a triangular bipyramid (symmetry C_{3v}), the next one (c) consists of an Ag^+ atom appended to Ag_2Br_2. It is not planar, the BrAg tail having an angle of 49 deg with the rhombus plane. Isomer (c) is the lowest one when using LCPs. We notice here a difference with the geometry of alkali halide ions which often occur to be C_∞ linear chains. In the case of $Cs_3I_2^+$, the bi-pyramid structure (b) is, however, degenerate with the linear chain.[30]

The lowest isomer of $Ag_4Br_3^+$ has C_{2v} symmetry and can be obtained from cyclic $Ag_3Br_3(D_{3h})$ by substituting one edge by a slightly folded rhombus bridge. The $Ag\widehat{Br}Ag$ angle opposite to the bridge is 75 deg, the AgBrM angles (where M is the middle of the AgAg bridge) are 76 deg. Hence, the replacement of a single atom by a pair does not strongly distort the cycle and the AgBr distances (4.79, 4.92, and 5.13 starting from the Br atom opposite to the bridge) are close to those in the D_{3h} Ag_3Br_3 structure. The geometry of the bridging rhombus ($d_{AgAg}=5.67$ bohr, $Ag\widehat{Br}Ag=72$ deg) is similar to that of Ag_2Br_2 (5.41 bohr and 65 deg, respectively). Isomer (b) results from parent Ag_4Br_4 (b) in which the tail Br^- ion was removed. It is actually geometrically extremely similar to structure (b) of $Ag_4Br_4^+$ (the angle of the Ag^+ tail with the Ag_3Br_3 plane is 114 deg). The similarity of the two clusters is understandable since the tail bromine in the latter is essentially neutral and does not play a strong role in the bonding. Isomer (c) results from another parent cluster, Ag_4Br_4 (c), in which one bromine ion was removed from one the C_{3v} axis. The AgBr distance linking the axis Ag atom to the three equivalent bromine is 5.58 bohr whereas the peripheric ones are 4.95 bohr. The peripheral $Br\widehat{Ag}Br$ angle is 111 deg instead of 107 in the parent cluster. It is interesting to remark that the distance between the three Ag atoms around the defect is large (7.52 bohr), which can be correlated with the absence of the stabilizing bromine anion. Finally, isomer (d) is the next member in the serie including Ag_2Br^+ and $Ag_3Br_2^+$(a). It is again alternant, and the $Ag\widehat{Br}Ag$ angles are further decreased (99 deg for the center angle, 103 deg for the other angles) with respect to the smaller species. It is interesting to notice that this structure is also a constituent linearized piece of cyclic Ag_6Br_6(a) (the equivalent angles are 94 deg). The Ag–Ag distances tend to decrease with size for the chains (7.93 bohr in Ag_2Br^+,7.62 bohr in $Ag_3Br_2^+$, 5.73 for the central one and 6.65 bohr for the two others in $Ag_4Br_3^+$). This reflects a collective effect along the axis containing the silver atoms, enhanced by the participation of $4p$ orbitals of bromine as discussed above for $Ag_3Br_2^+$(a). The Ag–Ag distance is 6.96 bohr in the hexamer cycle. All of these isomers for $Ag_4Br_3^+$ do exist in the LCP calculations; the lowest one corresponds to structure (c).

Only isomers (a), (b), and (c) were found stable in the SCP calculations for $Ag_5Br_4^+$. The lowest one is an open diedral structure consisting of two Ag_3Br_3 subunits sharing

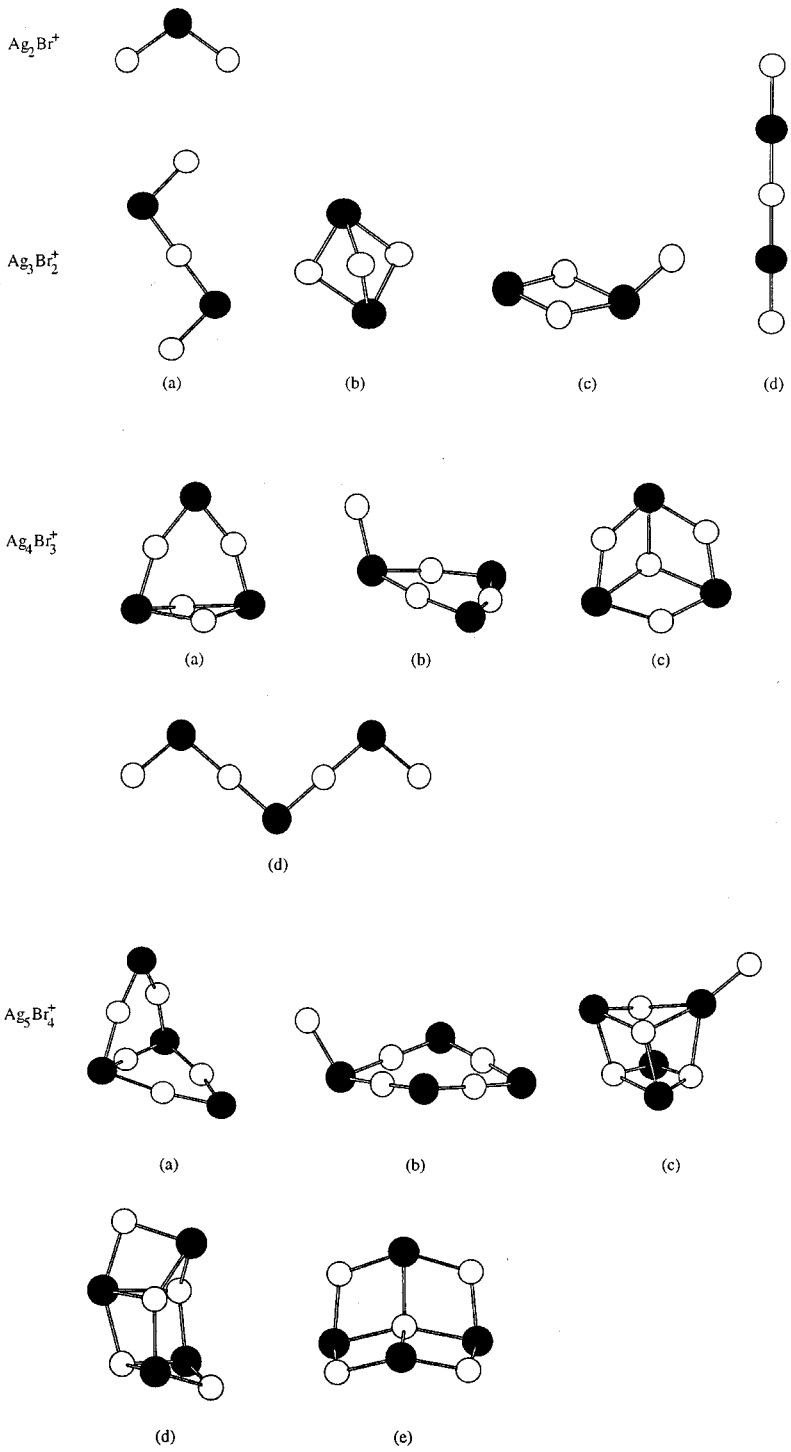

FIG. 3. Optimal geometries of cationic $Ag_nBr_{n-1}^+$ clusters.

an edge. The bond distances and the angles are very close to those of the isolated constituent ($d_{AgBr}=4.77$, 4.95, and 4.97 starting from the apex bromine and going to the central silver). The diedral angle is 100 deg which yields a separation of 7.41 bohr for the opposite silver atoms of the triangular units. The in-plane Ag–Ag distances are 5.92 bohr and 6.11 bohr (the latter involving the axis atom). Two isomers are located at 0.72 eV and 1.30 eV above (a). Isomer (b) has C_s symmetry and results from the addition of an Ag^+ ion to the Ag_4Br_4 square which is distorted into a rhombus with the Br–Br distances of 13.33 bohr in the C_s plane versus 9.83 bohr for the transverse one. The angle of the Ag^+ tail with the BrBr diagonal of the square is 121 deg. Structure (c) has C_{3v} symmetry and results from the addition of a silver ion to T_d neutral cluster Ag_4Br_4(c). In the LCP calculations, four isomers [(a), (c)–(e)] are almost degenerate within 0.3 eV, the lowest one being isomer (d).

Ag_nBr_{n-1} clusters were found to exhibit an electronic behavior essentially similar to that observed for alkali halide clusters with one excess metal atom, in the sense that all external electron of the metallic site are mainly transferred to the halogens except that of the extra silver atom. One is thus left with a so-called excess electron which occupies the HOMO orbital. The localization of this excess electron in

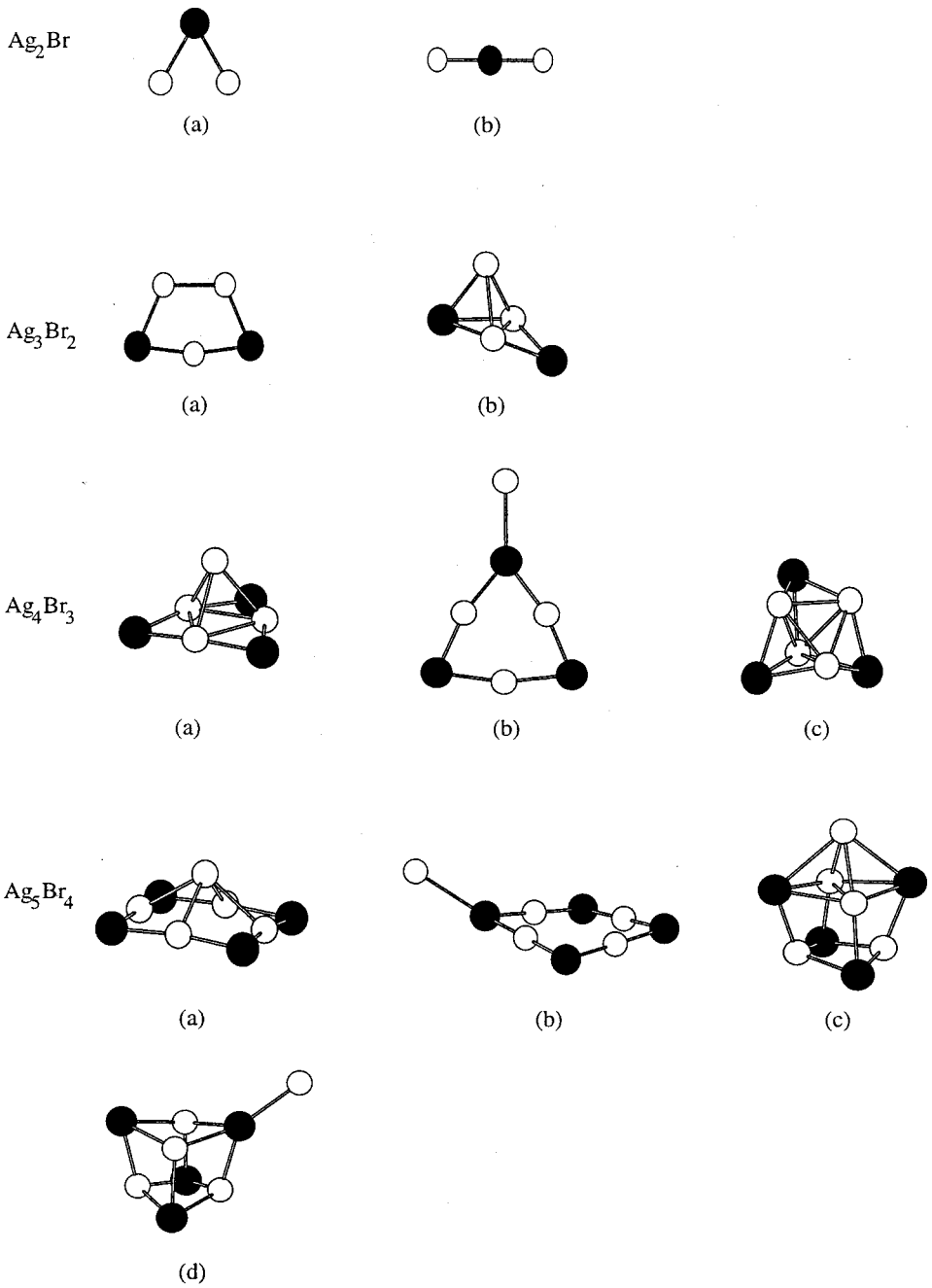

FIG. 4. Optimal geometries of neutral Ag_nBr_{n-1} clusters.

various clusters, whose density contour plots are shown in Figs. 5 and 6, will be discussed hereafter. Before examining this point, one should mention that the actual geometries (see Fig. 4 and Table IV) should turn out to differ significantly since the basic structures of stoichiometric Ag_nBr_n and $Ag_nBr_{n-1}^+$ are very different from those of the equivalent alkali halide systems.[3,29]

The lowest-energy isomer of Ag_3Br_2 is a planar pentagon (a) in which the excess electron localization is intermediate between two situations: (i) the first one where the electron would replace the missing bromine with respect to Ag_3Br_3; (ii) the second one where it would localize between the two connected Ag atoms, forming an Ag_2^+-like bond. Thus one can only partially consider it as an F-center localization. This is certainly due to the rather large strength of the Ag_2^+ bond and its balance in the cluster with purely electrostatic stability. One can notice that the Ag–Ag distance is significantly shorter than the second neighbor Ag–Ag distances in regular cluster Ag_3Br_3, for instance ($5.20a_0$ instead of $5.86a_0$). The presence of the excess electron in Ag_3Br_2 occurs to screen the Ag^+–Ag^+ repulsion, accordingly shortening the inter-silver distances. A second isomer (b) is found with a relative energy above structure (a) of 0.72 eV. It has C_s symmetry and consists of a silver atom nonsymmetrically capping an Ag_2Br_2 rhombus. This is one rare case where SCPs and LCPs yield the same geometries and energetical order. The structural LCP excitation energy is, however, half (0.30 eV) that obtained with SCPs.

The Ag_4Br_3 isomers exhibit two variations for an extra silver atom added to Ag_3Br_3(a). In isomer (a) with C_{3v} symmetry the extra silver atom lies on the axis above the triangular basis unit. The excess electron is essentially localized

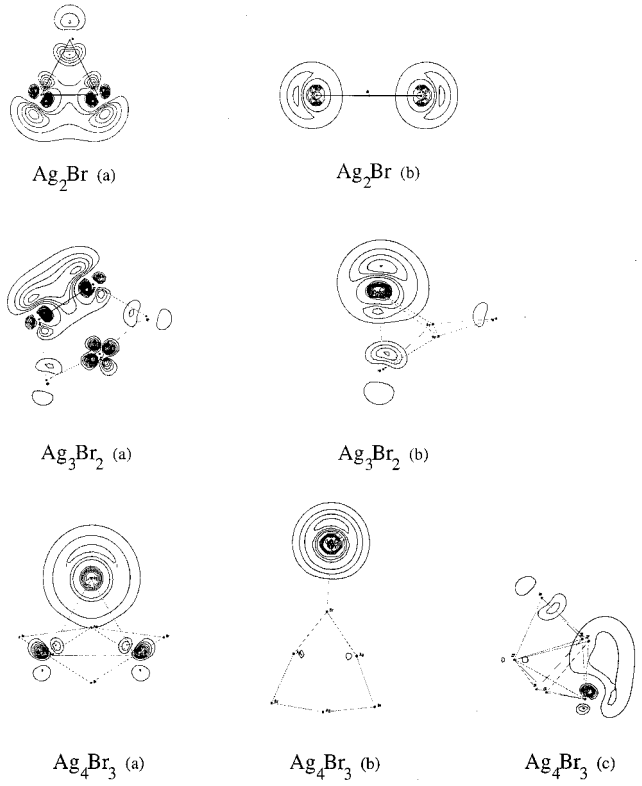

FIG. 5. Density contour plot of the excess electron orbital in Ag_nBr_{n-1} clusters for $n=2$, 3, and 4.

on the capping atom with very small tails on neighboring silver atoms of the triangular basis. In isomer (b), 0.31 eV above the former, the extra atom is appended to a bromine apex and is the equivalent of the so-called alkali atom tail demonstrated in studies for alkali halide clusters.[3,29] The excess electron is completely localized on the Ag tail atom. This is similar to what has been described elsewhere for Na tail electronic localization in Na_nF_{n-1}, either in cubiclike or hexagonallike patterns.[3] Due to the screening, the AgBr tail occurs to be significantly longer (5.97 bohr) than the AgBr lengths in the slightly C_{2v} distorted Ag_3Br_3 subunit (respectively, 4.85, 4.83, and 4.83 bohr starting from the tail bromine atom). This distance can also be compared to the equivalent length (4.85 bohr) in $Ag_4Br_3^+$(b). Finally, a third isomer (c) is found 0.73 eV above structure (a), which is obviously related to the T_d stoichiometric species Ag_4Br_4(c) or to the ionic species $Ag_4Br_3^+$(c). Here again, the excess electron localization is intermediate, between that of a metallic three-center bond and that of an F-center situation where the electron would replace the missing bromine. The inter-silver distance of the three Ag atom neighboring the electron is 5.42 bohr, much smaller than the equivalent distance (7.52 bohr) in $Ag_4Br_3^+$(c), clearly illustrating the screening role of the added electron. When LCPs are used, isomer (c) is the lowest, whereas the next one energetically is isomer (a), 0.05 eV higher, and the highest one is isomer (b) at 0.27 eV.

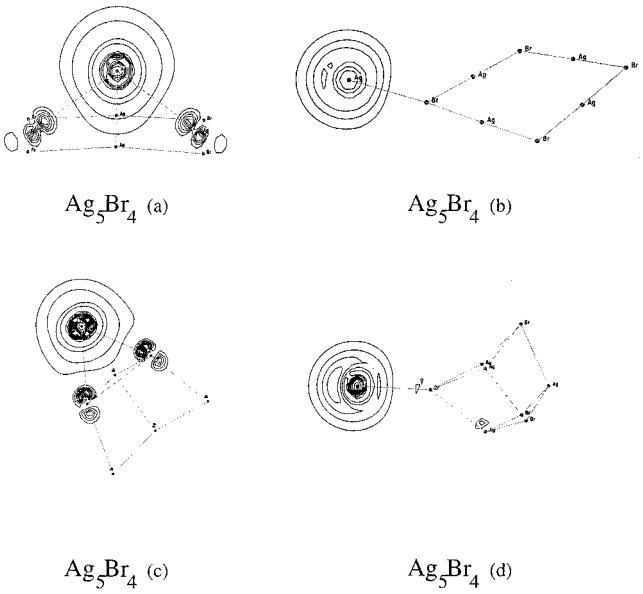

FIG. 6. Density contour plot of the excess electron orbital in Ag_5Br_4 isomers.

The lowest isomer of Ag_5Br_4(a) can be viewed as the addition of a silver atom on the axis of Ag_4Br_4(a) and has therefore C_{4v} symmetry. Its distance with the four neighboring silver atoms is 5.55 bohr. The Ag_4Br_4 basis of this pyramid is now almost planar. The AgBr distances in the square are 4.83 bohr, instead of 4.78 bohr in the parent stoichiometric cluster. The $Ag\widehat{Ag}Ag$ angle in the median plane is 111 deg. The extra electron essentially localizes on the top silver atom. As for Ag_4Br_3, a second isomer (b) with the same parent is found with a side-appended silver atom. The AgBr distance is rather long, 6.19 bohr, instead of 4.86 bohr in the similar ionic cluster $Ag_5Br_4^+$(b). The cluster is, however, not planar. The angle labeling the deviation from planar shape is 29 deg. The AgBr distances in the almost square unit, starting from the bromine tail atom, are 4.79 and 4.77 bohr, respectively. The electron, as in the Ag_4Br_3(b) cluster, localizes completely on the silver tail. Isomer (c) of Ag_5Br_4 has C_{2v} symmetry. It lies 1.26 eV above isomer (a) and consists of a silver atom capping one face of a distorted Ag_4Br_4 cube. The excess electron is essentially localized on this extra Ag atom. The distances of the latter with the two silver atoms of the face are 5.38 bohr, close to those between the three Ag atoms around the defect in Ag_4Br_3(c). Finally, a fourth structure (d) was found with C_{3v} symmetry formed by an Ag tail attached to a distorted $Ag_4Br_4T_d$-like unit. This configuration, similar to the structural ground state of the fluorine sodium cluster Na_5F_4,[3] lies here at rather high energy (1.57 eV) above isomer (a). The length of the AgBr tail is 5.61 bohr. When LCPs are used, the energetical ordering is completely changed and occurs to be (c), (a), and (d) 0.15 eV higher, and finally (b) at 0.46 eV above (c).

C. Stabilities

The binding energy of stoichiometric Ag_nBr_n clusters can be defined with respect to the free Ag^+ and Br^- ions, namely

$$\Delta_1(n)=\frac{1}{n}[-E(Ag_nBr_n)+nE(Ag^+)+nE(Br^-)].$$

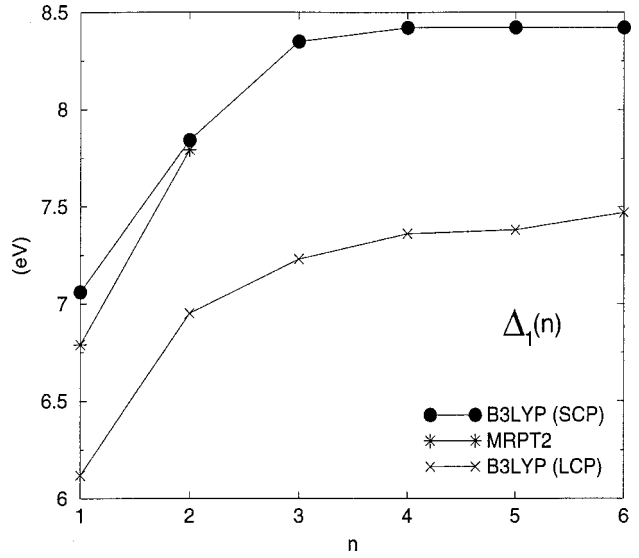

FIG. 7. Binding energy per ion in Ag_nBr_n clusters Δ_1 as a function of size. B3LYP (SCP): filled circle; B3LYP (LCP): cross; MRPT2 (from Ref. 12): star.

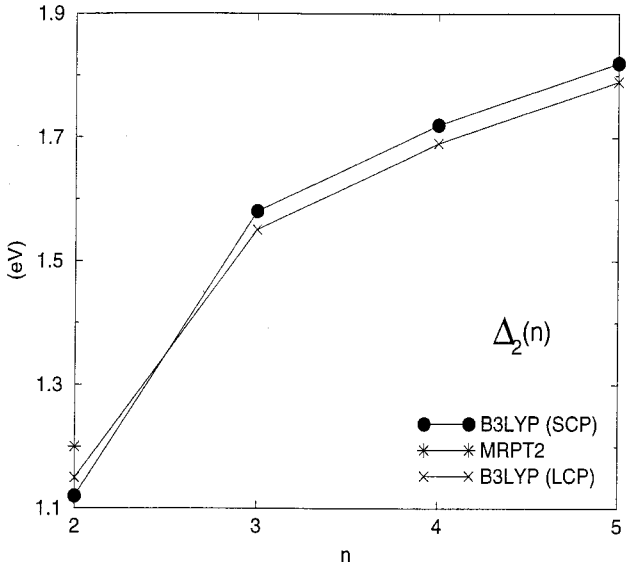

FIG. 8. Binding energy per atom in Ag_nBr_{n-1} clusters Δ_2 as a function of size. B3LYP (SCP): filled circle: B3LYP (LCP): cross; MRPT2 (from Ref. 12): star.

This binding energy is reported in Fig. 7 together with the previous MRPT2 results.[12] At all levels of approximation, the binding energy increases rather quickly up to $n=3$ and seems to show a slower increase as a function of size for $n>3$. No size appears to be particularly stable with respect to the neighboring ones, except $n=3$ which would be favored considering the second difference $\Delta_1(n+1)-2\Delta_1(n)+\Delta_1(n-1)$. This is much more prononced with SCPs. The stability is larger with SCPs, apparently reaching 8.4 eV for $n=6$ whereas the LCPs value is only 7.5 eV. One should note that in each case, the curve has been determined using the respective structural ground state isomers. The experimental bulk value is 9.32 eV.[38]

We now discuss the stability properties of Ag_nBr_{n-1} clusters. The binding energy per atom is hereafter defined as

$$\Delta_2(n)=\frac{1}{2n-1}\times[-E(Ag_nBr_{n-1})+nE(Ag)+(n-1)E(Br)],$$

and is shown in Fig. 8. Both SCP and LCP results present a continuous increase as a function of the size between 1.0 and 1.8 eV. Although the structural isomers are strongly different, both curves show a similar quantitative behavior.

From the present calculated data, one can consider fragmentation into a number of channels implying smaller stoichiometric or nonstoichiometric clusters with one excess silver atom. The corresponding fragmentation energies for Ag_nBr_n or Ag_nBr_{n-1} and $Ag_nBr_n^+$ or $Ag_nBr_{n-1}^+$ are given in Tables VI and VII, respectively.

For neutral stoichiometric Ag_nBr_n clusters, fragmentation into AgBr is often one of the lowest channels (in the range 1.3–1.6 eV). Nevertheless channels implying larger fragment units such as Ag_2Br_2 or even Ag_3Br_3 also lie at rather low energy. For instance, in Ag_6Br_6, the two channels yielding AgBr and Ag_2Br_2 are close, with respective fragmentation energies of 1.37 and 1.17 eV. Moreover, the remarkable point is that symmetric dissociation into two Ag_3Br_3 units occurs to be the lowest channel with a weak fragmentation energy of 0.42 eV. One can furthermore stress the particular stability of the Ag_3Br_3 cluster ($D_e=2.30$ eV), almost as stable with respect to Ag_2Br_2+AgBr than the dimer itself with respect to Ag+Br. For this family of clusters, the use of LCPs yields a qualitatively equivalent ordering of the fragmentation channels with, however, an important quantitative difference for the stability of Ag_3Br_3, only of 1.66 eV in the latter, a result correlated with a higher fragmentation energy of Ag_6Br_6 into two trimer units.

The situation is much simpler in the case of neutral Ag_nBr_{n-1} clusters for which evaporation of a single Ag atom always turns out to be the lowest channel (in the range 0.3–1.1 eV). The next fragmentation channels lie about 1 eV higher. The lowest dissociation energy is reached for Ag_4Br_3 (silver tail case), the largest one for Ag_3Br_2. The LCP calculations provide a very similar picture, even quantitatively.

Singly charged $Ag_nBr_n^+$ clusters also display a rather simple fragmentation scheme in which this time the evaporation of Br is energetically more favorable (fragmentation energies in the range 1–1.5 eV). The ordering of the channels is the same using LCPs. One may, however, recall that the SCP fragmentation energy (1 eV) of $AgBr^+$ is about twice the LCP value (0.55 eV).

The fragmentation of $Ag_nBr_{n-1}^+$ clusters appears to be more contrasted. For Ag_2Br^+ and $Ag_3Br_2^+$ fragmentation into neutral AgBr is the lowest channel. However, for the largest sizes investigated here, fragmentation into neutral Ag_3Br_3 appears to be favored, by 0.1 eV in the case of $Ag_4Br_3^+$ and 0.6 eV in the case of $Ag_5Br_4^+$. This is certainly correlated with the particular stability of Ag_3Br_3. Although we have not investigated larger clusters of this family, the present results provide the ordering of the channels involved for $Ag_6Br_5^+$. Two of those channels are quasi-degenerates within 0.02 eV, namely $Ag_5Br_4^+ + AgBr$ and $Ag_3Br_2^+ + Ag_3Br_3$ slightly higher.

TABLE V. Symmetry and relative energies (in eV) for positively charged clusters B3LYP optimized structures using two core pseudopotential on silver. A dash means that the structure is not a minimum.

Cluster		Symmetry	$[Ag^{19+}]$	$[Ag^{11+}]$
$Ag_2Br_2^+$	a	$D_{2h}-C_{2v}$[a]	0.00	0.00
	b	C_s	0.13	0.38
$Ag_3Br_3^+$	a	C_{2v}	0.00	0.18
	b	C_s	0.43	0.00
$Ag_4Br_4^+$	a	D_{4h}	0.00	0.74
	b	C_s	0.47	0.83
	c	C_{2v}	0.74	0.00
Ag_2Br^+	a	C_{2v}	0.00	0.00
$Ag_3Br_2^+$	a	C_{2h}	0.00	-
	b	C_{3v}	0.20	0.00
	c	C_s	0.33	0.21
	d	$D_{\infty h}$	-	0.32
$Ag_4Br_3^+$	a	C_{2v}	0.00	0.20
	b	C_s	0.15	0.63
	c	C_{3v}	0.15	0.00
	d	C_{2v}	0.29	0.72
$Ag_5Br_4^+$	a	C_{2v}	0.00	0.19
	b	C_s	0.72	-
	c	C_{3v}	1.30	0.28
	d	C_s	-	0.00
	e	C_{4v}	-	0.13

[a]The structure of $Ag_2Br_2^+$ is a planar rhombus using the $[Ag^{19+}]$ core pseudopotential (D_{2h} symmetry). With the $[Ag^{11+}]$ core pseudopotential, the geometry is not planar and the symmetry is C_{2v}.

TABLE VI. B3LYP fragmentation energies (in eV) for the energetically lowest dissociation channels of neutral Ag_nBr_n and Ag_nBr_{n-1} clusters. Calculations have been performed using two pseudopotential on silver.

Parent	Fragments	$[Ag^{19+}]$	$[Ag^{11+}]$
AgBr	Ag+Br	2.61	2.71
	$Ag^+ + Br^-$	7.06	6.12
Ag_2Br_2	2×AgBr	1.56	1.68
	Ag_2Br+Br	3.42	3.65
Ag_3Br_3	Ag_2Br_2+AgBr	2.30	1.66
	Ag_3Br_2+Br	3.80	3.72
Ag_4Br_4	Ag_3Br_3+AgBr	1.55	1.62
	$2\times Ag_2Br_2$	2.29	1.61
	Ag_4Br_3+Br	4.43	3.94
Ag_5Br_5	$Ag_3Br_3+Ag_2Br_2$	1.35	1.29
	Ag_4Br_4+AgBr	1.36	1.34
	Ag_5Br_4+Br	3.40	3.78
Ag_6Br_6	$2\times Ag_3Br_3$	0.42	1.45
	$Ag_4Br_4+Ag_2Br_2$	1.17	1.49
	Ag_5Br_5+AgBr	1.37	1.83
	Ag_6Br_5+Br		3.81
Ag_2Br	AgBr+Ag	0.75	0.73
	Ag_2+Br	1.84	2.21
Ag_3Br_2	Ag_2Br_2+Ag	1.11	0.65
	Ag_2Br+AgBr	1.92	1.59
Ag_4Br_3	Ag_3Br_3+Ag	0.35	0.39
	Ag_3Br_2+AgBr	1.54	1.40
	$Ag_2Br_2+Ag_2Br$	1.90	1.32
Ag_5Br_4	Ag_4Br_4+Ag	0.57	0.27
	$Ag_3Br_3+Ag_2Br$	1.37	1.16
	$Ag_3Br_2+Ag_2Br_2$	1.75	1.23
	Ag_4Br_3+AgBr	2.39	1.50

TABLE VII. B3LYP fragmentation energies (in eV) for the energetically lowest dissociation channels of $Ag_nBr_n^+$ and $Ag_nBr_{n-1}^+$ clusters. Calculations have been performed using two pseudopotential on silver. We also report the fragmentation rates, when available, observed in recent experiment (Ref. 39).

Parent	Fragments	$[Ag^{19+}]$	$[Ag^{11+}]$	Expt.
$AgBr^+$	Ag^++Br	1.00	0.55	
$Ag_2Br_2^+$	Ag_2Br^++Br	1.07	0.81	
	$AgBr^+$+AgBr	2.16	2.10	
$Ag_3Br_3^+$	$Ag_3Br_2^+$+Br	1.21	0.79	
	$Ag_2Br_2^+$+AgBr	1.79	1.59	
	$Ag_2Br_2+AgBr^+$	2.39	2.01	
$Ag_4Br_4^+$	$Ag_4Br_3^+$+Br	1.48	0.76	
	$Ag_3Br_3^+$+AgBr	1.91	1.77	
	$Ag_3Br_3+AgBr^+$	1.99	2.13	
	$Ag_2Br_2+Ag_2Br_2^+$	2.14	1.69	
Ag_2Br^+	$AgBr+Ag^+$	2.10	1.85	100%
	$AgBr^+$+Ag	3.70	4.01	
$Ag_3Br_2^+$	Ag_2Br^++AgBr	1.65	1.60	100%
	$Ag_2Br_2+Ag^+$	2.18	1.78	
	$Ag_2Br_2^+$+Ag	3.19	3.51	
$Ag_4Br_3^+$	$Ag_3Br_3+Ag^+$	1.66	1.92	45%
	$Ag_3Br_2^+$+AgBr	1.78	1.81	55%
	$Ag_2Br_2+Ag_2Br^+$	1.87	1.74	
	$Ag_3Br_3^+$+Ag	3.18	3.73	
$Ag_5Br_4^+$	$Ag_3Br_3+Ag_2Br^+$	1.66	1.59	100%
	$Ag_4Br_4+Ag^+$	2.21	1.81	
	$Ag_4Br_3^+$+AgBr	2.25	1.51	
	$Ag_3Br_2^+$+Ag_2Br_2	2.32	1.65	
	$Ag_4Br_4^+$+Ag	3.37	3.47	
$Ag_6Br_5^+$	$Ag_5Br_4^+$+AgBr	Δ[a]	Δ'[a]+0.16	84%
	$Ag_3Br_2^+$+Ag_3Br_3	$\Delta+0.02$	$\Delta'+0.15$	16%
	Ag_2Br^++Ag_4Br_4	$\Delta+0.11$	$\Delta'+0.13$	
	$Ag_4Br_3^+$+Ag_2Br_2	$\Delta+0.53$	Δ'	
	Ag^++Ag_5Br_5	$\Delta+0.84$	$\Delta'+0.64$	

[a]The energy of $Ag_6Br_5^+$ is not known, nevertheless we can calculate the dissociation energy to a constant Δ in SCP and Δ' in LCP calculations, respectively.

It is to be noted that the LCP ordering is significantly different for $n>3$.

D. Ionization potentials

We now discuss the ionization potentials. We provide both the vertical (when the ion is at the geometry of the neutral) and the adiabatic (including the relaxation of the ion geometry) ionization potentials, hereafter labeled IPv and IPa, respectively, for Ag_nBr_n and Ag_nBr_{n-1} clusters (see Table III and Figs. 9 and 10).

We start with stoichiometric Ag_nBr_n clusters (Fig. 9). The IPv values obtained with SCPs decrease from 10.40 eV for $n=1$ to 9.09 eV for $n=6$, with a strong increase for $n=3$. Although naturally lower, the adiabatic values IPa show the same trend almost merging with the vertical values at $n=4$. This is in line with the fact that the global geometries are not strongly affected by the change in the number of electrons, presenting only small quantitative interatomic reorganization. The LCP IPv's values show a general identical behavior except for the enhancement at $n=3$ which is less marked. Thus the special stability of the Ag_3Br_3 cluster is correlative of a large ionization potential. One may remark

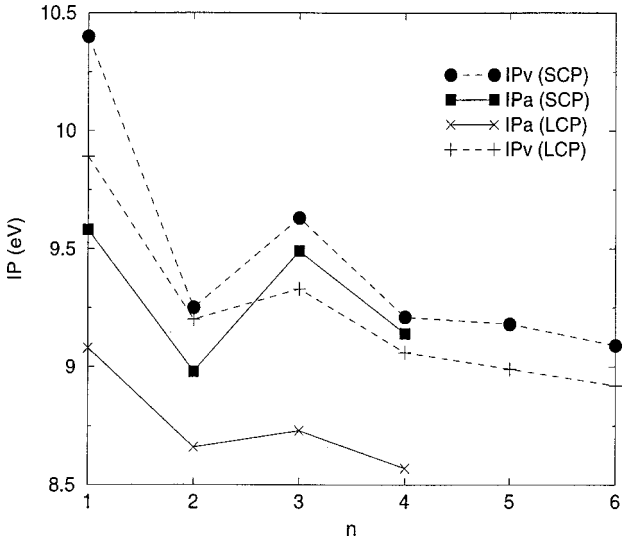

FIG. 9. B3LYP adiabatic (IPa) and vertical (IPv) ionization potential of Ag_nBr_n clusters. Dashed lines refer to IPv (filled circle: SCP calculation; cross: LCP calculation). Continuous lines refer to IPa (filled square: SCP calculation; cross: LCP calculation).

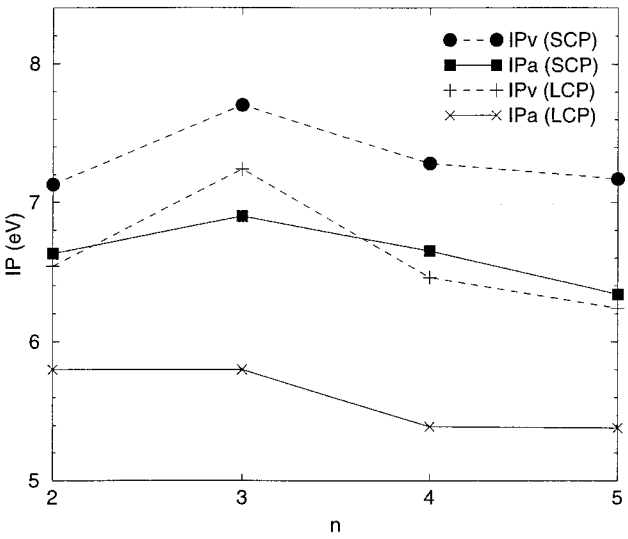

FIG. 10. B3LYP adiabatic (IPa) and vertical (IPv) ionization potential of Ag_nBr_{n-1} clusters. Dashed lines refer to IPv (filled circle: SCP calculation; cross: LCP calculation). Continuous lines refer to IPa (filled square: SCP calculation; cross: LCP calculation).

the enhanced one-electron level stability of the one-electron HOMO when using SCPs, 0.22 eV below the LCP value.

Those values (Table III) can be compared with the previous MRPT2 calculations (Table III), yielding namely IPv/IPa values of 9.00/8.84 eV for $n=1$ and 9.15/8.78 eV for $n=2$. An experimental estimate of 9.26 eV[36] is also available for AgBr, this latter between the SCP and LCP adiabatic DFT values.

The IPs of nonstoichiometric Ag_nBr_{n-1} (Fig. 10) are about 2–3 eV lower than those of stoichiometric Ag_nBr_n clusters. This reflects, whatever its detailed localization, the lower binding energy of the excess electron with respect to the case where the electron is involved in an ionic bonding. In both DFT calculations, IPv shows maxima for $n=3$ illustrating a stronger electronic localization on the Ag–Ag bond for this species. The maximum at $n=3$ is significantly smoothed in the adiabatic IP curve due to a complete geometry reorganization in the charged cluster with respect to the neutral species.

E. Dipole moments

The dipole moments are interesting observables, since they could in principle make possible discrimination between different isomers. For neutrals, the dipole moments corresponding to the low lying isomers are given in Table VIII. The clusters not reported in the table, namely Ag_2Br_2(a), Ag_3Br_3(a), Ag_4Br_4 (a) and (c), Ag_6Br_6(a–c), Ag_2Br(b) have a zero dipole moment due to symmetry.

The most important dipole moment is that of the AgBr dimer (5.34 Debye) with the exception of Ag_4Br_4(b) and Ag_5Br_5(d). The dimer value can be compared with the determination obtained using CCSD(T) calculations in large basis namely 7.13 Debye. We were unable to find any experimental value. Experimental data are, however, available for AgF and AgCl, respectively, 6.2 Debye and 5.73 Debye. Using the B3LYP dipole moment and the equilibrium internuclear distance $4.62a_0$ to compute the net charge of ions, one obtains a charge of 0.45, which is to be compared with corresponding Mulliken charge (0.39). Almost all the lowest-energy stoichiometric a clusters (a) have a vanishing dipole moment with the exception of Ag_5Br_5(a) where it is induced by the out of plane distorsion and anyway remains extremely small. It is interesting to analyze the influence on the dipole moment of the excess electron in Ag_nBr_{n-1} clusters. We have already discussed that the electron localization in Ag_2Br(a), Ag_3Br_2(a), and Ag_4Br_3(c) was intermediate between that of an F-center type localization and a partial two-center or three-center metallic bond. Those clusters result from a defect in an initially perfectly symmetric stoichiometric structure. The significant dipole moments for those three clusters (2.75, 2.82, and 2.23 Debye, respectively) confirm that, from the electrostatic point of view, the electron does not fully replace the missing bromine atom. Of course the extension of the electronic cloud with respect to a point charge might also be used as an argument in the same direction. Another effect influencing the dipole moment is the residual distortion of the remaining ions with respect to the perfectly symmetric structure. The dipole moments of clusters Ag_4Br_3 (a and b), Ag_5Br_4 (a–d), are noticeably smaller illustrating the important screening of the excess Ag^+ ion by the electron. It lies in the range 1–1.6 Debye when the extra atom caps a face, whereas it is even smaller (0.2–0.6 Debye) when one has a silver tail appended to an apex.

IV. CONCLUSION

The present calculations show that on the smaller clusters $Ag_nBr_p(n,p\leqslant 2)$, neutral or singly charged, the DFT-B3LYP calculations provide results comparable to more sophisticated methods belonging to the configuration interaction class, such as multi-reference CI plus second-order Moller–Plesset perturbation scheme or the coupled cluster method. This conclusion occurs to be true whatever

TABLE VIII. B3LYP dipole moment μ of neutral silver bromide clusters in Debye. Calculations have been performed using two pseudopotential on silver. The cluster not reported in the table, namely Ag_2Br_2 (a), Ag_3Br_3 (a), Ag_4Br_4 (a) and (c), Ag_6Br_6 (a–d), and Ag_2Br (b) have a zero dipole moment due to symmetry. A dash means that the structure is not a minimum.

Cluster		μ (Debye)	
		B3LYP [Ag^{19+}] core	B3LYP [Ag^{11+}] core
AgBr	a	5.34	7.10
Ag_3Br_3	b	-	6.46
Ag_4Br_4	b	6.32	-
Ag_5Br_5	a	0.16	0.27
	b	6.52	8.76
	c	1.23	2.18
	d	5.62	-
Ag_2Br	a	2.75	4.02
Ag_3Br_2	a	2.82	3.60
	b	2.11	2.47
Ag_4Br_3	a	1.57	2.27
	b	0.22	0.38
	c	2.23	3.11
Ag_5Br_4	a	1.06	0.95
	b	0.45	0.26
	c	1.27	0.79
	d	0.61	0.59

the pseudopotential used, SCP with 19 explicit electrons on silver atoms or LCP with 11 explicit electrons only.

On those small clusters, only minor geometrical differences were found when using LCP or SCP, except in the case of $Ag_2Br_2^+$. With LCP, this cluster occurs to be rhombus with longer AgAg diagonal, whereas the SCP calculation yields a rhombus with larger BrBr diagonal, close to a $BrAg_2^+Br$ configuration in agreement with the MRPT2 SCP finding in our previous work. An important effect of using SCP is to yield a dissociation energy of the $AgBr^+$ ion (1 eV) much closer to the experimental value 1.41 eV than the LCP value (0.55 eV). Therefore, it is expected that the SCPs will provide more accurate values of the fragmention energies, in particular for ions. SCPs also yield shorter AgBr distances, in average by 0.2 bohr with respect to LCP calculations. This SCP shrinking of the AgBr bond length is general for most clusters investigated here.

Ag_3Br_3 appears of particular significance in the present study. The shapes obtained with SCPs or LCPs are rather close, namely a deformed triangle. The silver atoms form an inner triangle with 5.86 bohr side whereas the bromine atoms point outward. One could assign this effect to polarization forces due to the large polarizability ratio of Br^- versus Ag^+. However, the SCP calculation shows an interaction and mixing between the $4d$ orbitals of silver and the $4p$ orbitals of bromine much larger than when LCPs are used.

Figure 11 illustrates such interactions. In the case of Ag_2Br^+, molecular orbital $(4)b_2$ shows the bond overlap of the $4p_{Br}$ and $4d_{Ag}$ between Ag and Br. Orbital $(5)a_1$ is a three-center molecular orbital with bonding interaction of two silver d orbitals and one of the p orbital of bromine. Those two molecular orbital situations can also be observed on Ag_3Br_3 [see molecular orbitals $(9)a_2'$ and $(4)a_1'$]. It can be noticed that the interaction $4p_{Br}4d_{Ag}4p_{Br}$ yielding molecular orbital $(9)a_2'$ tends to favor BrAgBr alignment and thus has a geometric influence in this case similar to that of polarization contribution. The interaction yielding molecular orbital $(4)a_1'$ tends to restaure some density between pairs of silver atoms. Even three-center cooperative bonding can be obtained such as for instance in orbital $(5)a_1'$.

Clearly, this important mixing is mediated by the presence of the inner semi-core $4s$ and $4p$ electrons of silver, explicit in the SCP scheme, which play here a quantitative role, although the intervention of those semi-core orbitals is not directly visible in the orbital pictures. Actually the SCP calculation yields a stability for Ag_3Br_3 much larger than that obtained with LCPs (dissociation energy of 2.30 eV versus 1.66 eV). Therefore, the stronger $4p/4d$ mixing enhances the strength of the bonding character of the MOs and decreases that of the antibonding ones, resulting in an increase of the total stability of the cluster.

For larger stoechiometric clusters $Ag_nBr_n(n \leqslant 6)$, the ordering of the geometries obtained with 19-electron pseudopotentials are very different from those obtained with 11-electron pseudopotentials. It appears that cyclic arrangements are favored. However, except for $n=3$, those cycles are not planar and the silver atom tend to shorten their interatomic separations (6.65 bohr in Ag_4Br_4, 6.82–7.25 bohr in Ag_5Br_5, 6.96 bohr in Ag_6Br_6) with respect to what it would be in planar cycles. Oppositely the bromine atoms generally point outward. There is a strong BrAgBr alignment which is due to the same $4p_{Br}4d_{Ag}4p_{Br}$ interaction whereas the AgBrAg angles are always in the range 90–110 deg. The same features can be found in the next stoichiometric isomers with geometries in which the previous Ag_3Br_3 and Ag_4Br_4 can often be identified as building units. Thus the stoichometric clusters found here exhibit very different geometric and electronic properties than those reported in alkali halide clusters (generally exhibiting cubiclike or hexagonal arrangements). As an example, isomer Ag_4Br_4 (c) which corresponds to a T_d distorted a cube, and which is energetically the lowest one with LCPs is only the third one with SCPs at 1.07 eV above isomer (a).

The global shapes of the lowest stoichiometric clusters is only poorly affected by the removal of one electron. The result is generally to increase the AgAg separation (from 5.41 to 6.47 bohr for $n=2$, from 6.65 bohr to 7.04 bohr for $n=4$). In case $n=3$, the situation is complicated by a Jahn–Teller effect.

The Ag_nBr_{n-1} clusters with an excess electron show essentially geometries corresponding to the addition of the extra silver atom to one of the existing stoichiometric Ag_nBr_n isomers. In the lowest-energy isomers, again Ag_3Br_3 and Ag_4Br_4 are important basic supports for such addition. Although one often observes an apparent innercluster segregation of the silver atoms, the excess electron essentially localizes on the extra silver atom. Some isomers exhibit situations closer to those observed in alkali halide clusters with one excess alkali atom, such as silver tails [Ag_4Br_3 (b), Ag_5Br_4 (b) and (c)], appended, however, here on a different supporting subcluster. Finally F-center type defects where the electron replaces a missing bromine atom also exist such as in Ag_3Br_2 (a) and Ag_4Br_3 (c). However, the situation is somewhat more complex in silver bromide since the extra electron

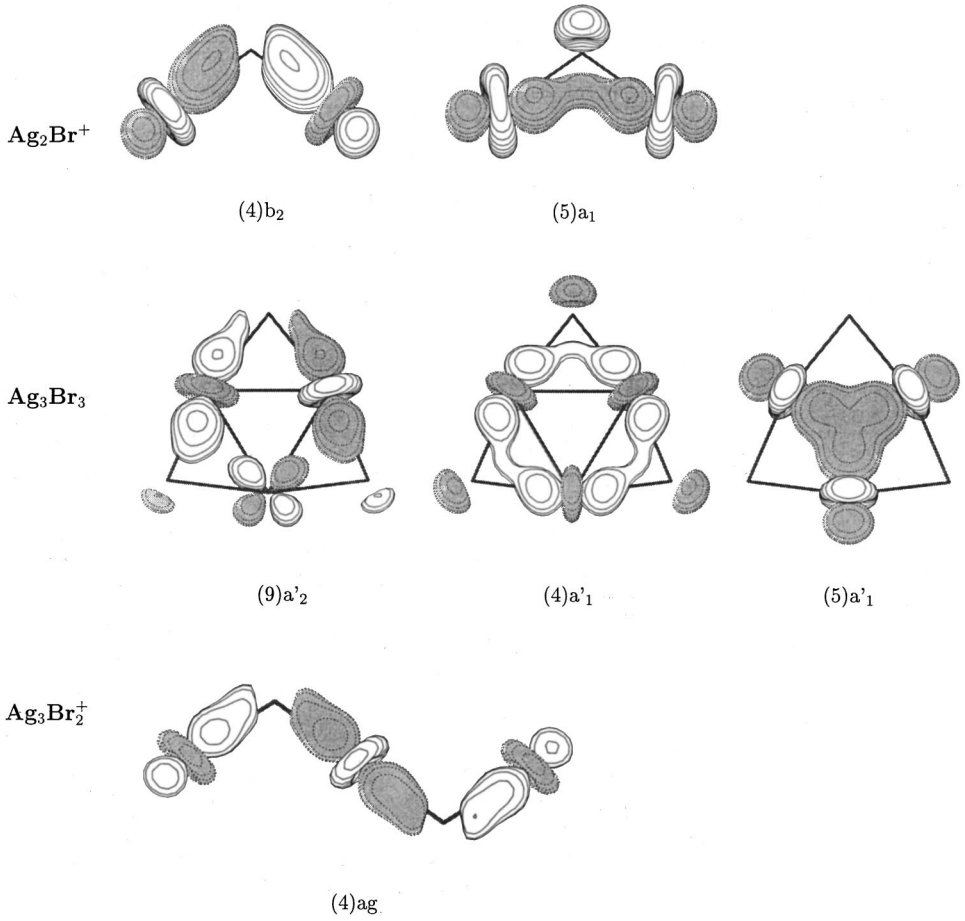

FIG. 11. Molecular orbitals contour plots of Ag_2Br^+, Ag_3Br_3, and $Ag_3B_2^+$.

tends to be closer to the two or three neighboring silver atoms, thus presenting an intermediate case between a pure F-center (electrostatic stability) and a two-center or three-center metallic bond.

$Ag_nBr_{n-1}^+$ exhibit a systematic and important relaxation with respect to the neutral species. Triangular subunits still play an important role. A peculiar geometry is obtained for $Ag_5Br_4^+$ (a) consisting of two connected Ag_3Br_3 units. However, the originality lies in the obtention of open zigzag chains with rigid linear BrAgBr units [$Ag_3Br_2^+$ (a), $Ag_4Br_3^+$ (d)], extending the Ag_2Br^+ structure.

The fragmentation energies of the clusters appears to be dominated by essentially one channel in two cases: $Ag_nBr_n^+$ clusters almost always evaporate a neutral bromine atom, Ag_nBr_{n-1} clusters evaporate a silver atom. The situation is more complex for stoichiometric clusters where several channels may be in competition from an energetical point of view. Dissociation into AgBr is the lowest for $n \leqslant 4$, that into Ag_3Br_3 is lower for $n > 3$. Such competition is also observed for $Ag_nBr_{n-1}^+$ clusters. It must be emphasized that in the latter case, SCP calculations provide for $n > 3$ the lowest dissociation channel as that corresponding to Ag_3Br_3, contrary to the LCP calculations. Interestingly, fragmentation of $Ag_nBr_{n-1}^+$ clusters has been investigated very recently by some of us in mass-selective supersonic beam experiments. Those investigations will be the object of a specific publication.[39] However, the fragmentation rates obtained are listed in Table VII, together with the calculated fragmentation energies. Ag_2Br^+ and $Ag_3Br_2^+$ yield a unique fragmentation channel, respectively, Ag^+ and Ag_2Br^+ (only the fragment ions are detected in experiment). For the former fragmentation, both SCP and LCP favor a single channel around 2 eV. In the latter case, the LCP calculations predict two channels to be very close (1.60 and 1.78 eV, respectively), whereas the SCP calculation find the observed experimental channel $Ag_2Br^+ + AgBr$ to lie 0.53 eV below $Ag_2Br_2 + Ag^+$. In the case of $Ag_4Br_3^+$, two channels are actually observed, with rates around 45/55. This agrees better to the energetical ordering predicted by the SCP calculation. In $Ag_5Br_4^+$, the SCP calculation predicts $Ag_2Br^+ + Ag_3Br_3$ as the lowest channel, 0.5 eV below the next higher ones, whereas in the LCP calculation, three and even four channels are close lying. The experiment only exhibits one channel corresponding to the lowest SCP one. In the case of $Ag_6Br_5^+$, two channels are observed with rates around 84/16. Again, this agrees better to the energetical ordering predicted by the SCP calculation. Thus it seems that, as already shown on $AgBr^+$, the fragmentation energetics is better obtained in the SCP calculation. One should, however, remain aware that the present analysis neglects possible kinetic effects in the fragmentation processes.

The present work has illustrated that the conformations and stability patterns of silver halide clusters is not reductible

to those found for simpler ionic systems such as the alkali halide clusters. For the smallest neutral stoichiometric species up to $n=3$, the present results agree fairly well with those of Srinivas *et al.*[18] and Zhang *et al.*[17] In the case of $Ag_2Br_2^+$, Srinivas *et al.* mention a reversal of the Ag–Ag distance versus the Br–Br one with respect to the neutral cluster. Our SCP calculation does not provide such a change in agreement with our previous MRPT2 calculation but conversely to the present LCP result. For the larger clusters ($n \geqslant 4$) the structures proposed by the other authors correspond to structurally excited isomers Ag_4Br_4 (c), Ag_5Br_5 (c), and Ag_6Br_6 (c). However, the cyclic structures appear in the present work to be lower in the energy than the former isomers.

To check the reliability of the present results, and in particular that no artifact was induced by the pseudopotentials, we have achieved for the Ag_4Br_4 cluster all-electron B3LYP gradient calculations. We have tested small basis sets such as those used by Zhang *et al.*[17] comparing the cyclic C_{2v} isomer and the T_d one. Both were found as stable structures and the latter was energetically lower. We then repeated the calculations using larger basis sets, up to a final completely uncontracted set including $17s13p8d1f$ on silver and $12s11p4d$ on bromine. With this extensive basis, we found that the cyclic C_{2v} isomer is below the T_d structure by 0.35 eV. The crucial factor is not the f function and the actual final ordering is already obtained when decontracting the valence functions and adding some diffuse s and p functions on bromine and silver atoms. This corresponds to the quality of the basis set used in our SCP calculations. As in the calculation of Zhang *et al.*, the present all-electron calculation is nonrelativistic, which as previously mentioned, might be questioned for atoms such as bromine or silver. It nevertheless emphasizes the crucial necessity of sufficiently flexible and extended basis sets, especially in the valence and semi-valence region. It is also possible that the cyclic structures were not reached by the local search gradient procedures of Zhang *et al.*[17] and Srinivas *et al.*[18] Interestingly, for some of the species investigated here, the results are very similar to those obtained by Bertolus *et al.*[31] on $Ag_n(OH)_n$ and $Ag_n(OH)_{n-1}^+$ clusters ($n \leqslant 4$) who also found a cyclic structure for $Ag_4(OH)_4$. Moreover this cyclic pattern is consistent with early infrared absorption spectra of matrix-isolated noble metal halides (Ref. 40) assigned by the authors as originating from eight-atom rings for $(CuCl)_4$ and planar geometries for $(CuBr)_{6,7,8}$.

We hope to stimulate experimental investigations on those systems, such as the observation of ionization potentials which have not yet been measured, probably because they lie in the UV region, which is not easily accessible. The theoretical investigations should also be completed by the extension to larger clusters to understand the geometry transition to the cubic regime. Also, partioning of the chemical contributions to the energy in such small clusters should be quantitatively investigated in order to design adequate models to describe the forces and to be used in extensive dynamical or thermodynamical simulations.

ACKNOWLEDGMENT

The calculations were achieved thanks to computer time allocation in the CALMIP project at the Centre Inter Universitaire de Calcul (CICT) Toulouse.

[1] U. Landman, D. Scharf, and J. Jortner, Phys. Rev. Lett. **54**, 1860 (1985).
[2] J. Rajagopal, R. N. Barnett, A. Nitzan, U. Landman, E. C. Honea, P. Labastie, M. L. Homer, and R. L. Whetten, Phys. Rev. Lett. **64**, 2933 (1990).
[3] G. Durand, J. Giraud-Girard, D. Maynau, F. Spiegelmann, and F. Calvo, J. Chem. Phys. **110**, 7871 (1999).
[4] G. Durand, F. Spiegelmann, Ph. Poncharal, P. Labastie, J. M. L'Hermite, and M. Sence, J. Chem. Phys. **110**, 7884 (1999).
[5] P. Fayet, F. Granzer, G. Hegenbart, E. Moisar, B. Pischel, and L. Woste, Z. Phys. D: At., Mol. Clusters **3**, 299 (1986).
[6] M. Mostafavi, J. L. Marignier, J. Amblard, and J. Belloni, Z. Phys. D: At., Mol. Clusters **12**, 31 (1989).
[7] R. K. Hailstone and D. E. Erdtmann, J. Appl. Phys. **76**, 4184 (1994).
[8] J. Flad, H. Stoll, and H. Preuß, Z. Phys. D: At., Mol. Clusters **6**, 193, 287 (1987).
[9] J. Flad, H. Stoll, A. Nicklass, and H. Preuß, Z. Phys. D: At., Mol. Clusters **15**, 79 (1990).
[10] R. C. Baetzold, J. Phys. Chem. **101**, 8180 (1997).
[11] R. Pou-Amérigo, V. Bonačić-Koutecký, and P. Fantucci, poster at the TAMC3 conference, Berlin, October 5–9, 1999.
[12] F. Rabilloud, F. Spiegelmann, and J. L. Heully, J. Chem. Phys. **111**, 8925 (1999).
[13] C. R. A. Catlow, J. Corish, J. H. Harding, and P. W. M. Jacobs, Philos. Mag. A **55**, 481 (1987).
[14] L. Jansen and E. Lombardi, Phys. Rev. Lett. **12**, 11 (1964).
[15] N. T. Wilson, M. Wilson, P. A. Madden, and C. Pyper, J. Chem. Phys. **105**, 11209 (1996).
[16] C.-H. Kiang and W. A. Goddard III, J. Phys. Chem. **99**, 14334 (1995).
[17] H. Zang, Z. A. Schelly, and D. S. Marynick, J. Phys. Chem. A **104**, 6287 (2000).
[18] S. Srinivas, U. A. Salian, and J. Jellinek, in *Metal-Ligand Interactions in Chemistry, Physics and Biology*, edited by N. Russo and D. R. Salahub (U.S. Gouvernment, Printed in The Netherlands, 2000), pp. 295–324.
[19] P. J. Hay and W. R. Wadt, J. Chem. Phys. **82**, 270 (1985).
[20] V. Bonačić-Koutecký, J. Pittner, M. Boiron, and P. Fantucci, J. Chem. Phys. **100**, 3876 (1999).
[21] V. Bonačić-Koutecký, M. Boiron, J. Pittner, P. Fantucci, and J. Koutecký, Eur. Phys. J. D **9**, 183 (1999).
[22] D. Andrae, U. Háussermann, M. Dolg, H. Stoll, and H. Preuss, Theor. Chim. Acta **77**, 123 (1990).
[23] L. Mahé, Ph. D. thesis, Université Paul Sabatier, Toulouse, France, 1997.
[24] A. Bergner, M. Dolg, W. Kuchle, H. Stoll, and H. Preuss, Mol. Phys. **80**, 1431 (1993).
[25] A. Ramirez-Solis, J. P. Daudey, O. Novaro, and M. E. Ruiz, Z. Phys. D: At., Mol. Clusters **15**, 71 (1990).
[26] GAUSSIAN 98, Revision A.6, M. J. Frisch, G. W. Trucks, H. B. Schlegel, G. E. Scuseria, M. A. Robb, J. R. Cheeseman, V. G. Zakrzewski, J. A. Montgomery, Jr., R. E. Stratmann, J. C. Burant, S. Dapprich, J. M. Millam, A. D. Daniels, K. N. Kudin, M. C. Strain, O. Farkas, J. Tomasi, V. Barone, M. Cossi, R. Cammi, B. Mennucci, C. Pomelli, C. Adamo, S. Clifford, J. Ochterski, G. A. Petersson, P. Y. Ayala, Q. Cui, K. Morokuma, D. K. Malick, A. D. Rabuck, K. Raghavachari, J. B. Foresman, J. Cioslowski, J. V. Ortiz, B. B. Stefanov, G. Liu, A. Liashenko, P. Piskorz, I. Komaromi, R. Gomperts, R. L. Martin, D. J. Fox, T. Keith, M. A. Al-Laham, C. Y. Peng, A. Nanayakkara, C. Gonzalez, M. Challacombe, P. M. W. Gill, B. Johnson, W. Chen, M. W. Wong, J. L. Andres, C. Gonzalez, M. Head-Gordon, E. S. Replogle, and J. A. Pople, Gaussian, Inc., Pittsburgh, PA, 1998.
[27] A. D. Becke, J. Chem. Phys. **98**, 5648 (1993).
[28] F. Calvo, Ph. D. thesis, Université Paul Sabatier, Toulouse, France, 1998.
[29] V. Bonačić-Koutecký, J. Pittner, and J. Koutecky, Chem. Phys. **210**, 313 (1996).
[30] A. Aguado, A. Ayuela, J. M. López, and J. A. Alonso, Phys. Rev. B **58**, 9972 (1998).

[31] M. Bertolus, V. Brenner, and P. Millie, Eur. Phys. J. D **11**, 387 (2000).
[32] V. Beutel, H.-G. Krämer, G. L. Bhale, M. Kuhn, K. Weyers, and W. Demtröder, J. Chem. Phys. **98**, 2669 (1993).
[33] M. D. Morse, Chem. Rev. **86**, 1049 (1986).
[34] K. P. Huber and G. Herzberg, ''Molecular spectra and molecular structure,'' *Constants of Diatomic Molecules* (Van Nostrand Reinhold, New York, 1979), Vol. 4.
[35] K. P. R. Nair and J. Hoeft, Phys. Rev. A **35**, 668 (1987).
[36] J. Berkowitz, C. H. Batson, and G. L. Goodman, J. Chem. Phys. **11**, 5829 (1980).
[37] E. R. Cohen and B. N. Taylor, J. Phys. Chem. Ref. Data **17**, 1795 (1988).
[38] C. D. Thurmond, J. Am. Chem. Soc. **75**, 3928 (1953).
[39] J. M. L'Hermite, F. Rabilloud, L. Marcou, and P. Labastie (unpublished).
[40] T. P. Martin and H. Schaber, J. Chem. Phys. **73**, 3541 (1980).